Online ISSN: 2228-6233 Print ISSN: 2228-6225

Received: 14- Februray-2026

Revised: 16- May -2026

Accepted: 17- May-2026

DOI: https://doi.org/10.57647/ijm2c.2027.1701.03

ORIGINAL RESEARCH

A hybrid numerical approach for Volterra integro-differential equations via Block-Pulse and Müntz functions

Parvin Badihian[a], Majid Tavassili Kajani[a,*]

May 17, 2026

[a] *Department of Mathematics, Isf.C., Islamic Azad University, Isfahan, Iran.*

Abstract

In this paper, we present a novel set of hybrid functions using the Block-Pulse functions and a new class of Müntz functions to obtain numerical solutions for Volterra integro-differential equations (VIDEs). In this method, by implementing the collocation approach based on the new hybrid basis as the trial functions, the given VIDE is reformulated as a system of algebraic equations. As opposed to the existing methods that use Müntz–Legendre polynomials, we utilize a new set of Müntz functions that have distinct real roots in the interval $[0, 1]$. Furthermore, the convergence, stability and accuracy of the method are studied. Numerical examples are included to demonstrate the efficiency and high accuracy of the proposed approach.

Keywords: Müntz functions; Block-Pulse functions; Collocation method; Volterra integro-differential equation; Convergence; Stability.

1 Introduction

In recent decades, integro-differential equations have attracted special attention due to their application in modeling a wide range of physical and engineering problems such as fluid dynamics [1], heat and mass transfer [2] and so on. Many studies on the development of accurate numerical methods for solving these equations have been done such as the Tau method [3, 4], wavelet-Galerkin method [5], Chebyshev collocation method [6–8], Lagrange interpolation method [9], spectral Legendre-Chebyshev method [10], power series method [11], Haar wavelet method [12], operational matrix with Block-Pulse functions [13], operational matrix with Hat functions [14], Legendre polynomials method [15] and physics-informed deep AI simulation [16].

Volterra integro-differential equations (VIDEs) have also been solved using emerging numerical strategies, which are described below. The hybrid multistep method has been used in [17] to address VIDEs. The ANNs approach has been employed in [18] to solve fractional order VIDEs. Two-dimensional fractional-order VIDEs have been investigated in [19]. Fractional higher-order linear VIDEs are studied in [20]. In [21], the A-PINN (auxiliary physics informed neural networks) approach has been implemented to solve the forward problems involving nonlinear VIDEs system, nonlinear 2-dimensional VIDE and nonlinear 1-dimensional VIDEs. In [22], a spectral technique has been used to address variable-order fractional VIDEs. An algorithm for solving VIDEs based on Alperta's multi-wavelets Galerkin method is presented in [23]. A fast sparse spectral method has been utilized in [24] for nonlinear VIDEs with general kernel.

Additionally, the authors of [25] discuss the numerical solution of fuzzy Fredholm-Volterra integro-differential equations by the reproducing kernel algorithm. The work done in [26], addresses the solution of fuzzy fractional Volterra and Fredholm integro-differential equations using adaptation of kernel functions based approach with Atangana-Baleanu-Caputo distributed order derivative. In [27], the authors investigate the well-posedness of Caputo-Fabrizio fractional stochastic integro-differential equations employing Legendre-spectral approach. In [28] the existence, uniqueness, and collocation solutions using the shifted Legendre spectral method for the Hilfer fractional stochastic integro-differential equations regarding stochastic Brownian motion have been investigated.

*Corresponding author, *E-mail address*: mtavassoli@iau.ac.ir

Müntz functions were first introduced by Badalyan [29] and Taslakyan [30]. The properties of these functions were explored by McCarthy et. al. [31] and completed by Borwein et. al. [32]. In general, there exist two class of Müntz polynomials that are orthogonal concerning certain inner products. The first class is referred to as Müntz–Legendre polynomials as is defined in (3.2). They involve the real powers of τ and are related to a class of fractional Jacobi functions. The second class was defined in [33, 34] and are called Müntz functions. They involve integer powers of τ together with the ln function and have distinct real roots in the interval $[0, 1]$ (see Section 3 for further details).

So far, Müntz–Legendre polynomials have been widely utilized in the literature for solving various kinds of functional equations. They have been used in [35] to determine a numerical solution for the fractional Bagley-Torvik equation, in [36] for solving fractional differential equations through the collocation approach, in [37] to solve fractional differential equations with distributed order, in [38] for solving fractional differential equations using the Tau approach, in [39] for solving nonlinear fractional optimal control problems and in [40] for deriving solutions to Volterra-Fredholm integral equations. In addition, numerical solutions for fractional-order integro-differential equations utilizing a Müntz-Jacobi Tau method has been presented in [41]. Fredholm integral equations of the first kind are solved in [42] using Müntz wavelets and Volterra-Fredholm integro-differential equations are solved in [43] using a Müntz-Legendre wavelet approach.

In the current work, we are going to introduce a novel hybrid set of orthogonal functions called hybrid of Block-Pulse and Müntz functions and use it in solving the following class of VIDEs:

$$G_1\big(\tau, \psi(\tau), \frac{d\psi(\tau)}{d\tau}\big) = G_2\big(\tau, h(\tau), \psi(\tau), \int_0^\tau T(\tau, s)V\big(s, \psi(s)\big)ds\big), \qquad \tau \in \Gamma = [0, 1], \tag{1.1}$$

with the initial condition $\psi(\tau_0) = \xi$, where ξ is a given constant, G_1, G_2, h and V are known continuous functions on appropriate domains, $\psi(\tau)$ represents the unknown function that should be determined and $T(\tau, s)$ is a continuous kernel defined over the domain $\Gamma \times \mathbb{R}$.

Our numerical scheme for solving 1.1 is based on the domain decomposition strategy by utilizing the Block-Pulse functions and the collocation method using the roots of the Müntz functions. Instead of fractional powers of shifted Legendre–Gauss or Chebyshev–Gauss points, shifted Müntz points are employed as the collocation points in each subinterval. Convergence rate for function approximation using the proposed hybrid basis is assessed and the error and numerical stability of the suggested approach are analyzed.

For more convenience, all the symbols and functions used in the paper are summarized in 1. The rest of the paper is also organized as follows: In Section 2, we discuss some theorems that focus on the existence and uniqueness of the solutions for VIDEs. Section 3 includes essential and foundational preliminaries. In Section 4, we introduce a new hybrid function as the orthogonal basis for solving the VIDE (1.1). In Section 5, we present the numerical technique in details and present the algorithm of our method. In Section 6, the stability of the method is discussed and in Section 7, the error analysis has been given. Section 8, includes the relevant examples to show the validity and accuracy of our approach. Finally, conclusions and suggestions for future works are given in Section 9.

2 Existence and uniqueness of the solution

In this section, by using a theorem regarding the uniqueness of the solution of integral equations we investigate a theorem concerning existence and uniqueness of the solution of VIDEs.

Theorem 2.1. *Consider the Volterra integral equation presented below [44]:*

$$\psi(\tau) = h(\tau) + \int_0^\tau T\big(\tau, s, \psi(s)\big)ds, \tag{2.1}$$

and assume that
(1) $h \in C[0, 1]$,
(2) for $0 \le s \le \tau \le 1$ *and* $\|u\| < \infty$, $T\big(\tau, s, \psi(s)\big)$ *is continuous,*
(3) for $0 \le s \le \tau \le 1$, $T\big(\tau, s, \psi(s)\big)$ *satisfies the Lipschitz condition.*
Then, the equation (2.1) *has a unique solution.*

Table 1: Symbols and functions used in the paper.

Symbol	Explanation
$\psi(\tau)$	Unknown function of equation
$h(\tau)$	Known continuous function of equation
$T(\tau, s)$	Continuous kernel in terms of variables τ, s
$V\big(s, \psi(s)\big)$	Continuous function in terms of variables $s, \psi(s)$
$g_q(\tau)$	Müntz function of order q
$d_q(\tau), w_q(\tau)$	Algebraic polynomials in Müntz function
$\rho_w(\tau)$	Block-Pulse function of order w
$\varphi_{wq}(\tau)$	Hybrid function of Block-Pulse and Müntz functions
$L_N(\psi)$	Truncated series of Legendre polynomials for the function ψ
s_q	The qth root of the Müntz function
E_N	Residual error
$H^u(a, b)$	Sobolev space of integer order u on the interval (a, b)
$L^2(a, b)$	Space of square-integrable functions defined on the interval (a, b)
$C^{u-1}([a, b])$	Functions that are $u-1$ times differentiable and their $(u-1)$-th derivative is continuous on the interval $[a, b]$

Proof. Refer to [45]. □

Theorem 2.2. *Consider the Volterra integro-differntial equation* (1.1) *in the form specified below:*

$$\psi'(\tau) = h\big(\tau, \psi(\tau)\big) + \int_0^\tau T\big(\tau, s, \psi(s)\big)ds \tag{2.2}$$

with the initial condition $\psi(\tau_0) = \xi$. *If* h *and* T *be continuous functions and satisfy the Lipschitz condition i.e.,*

$$\|h\big(\tau, \psi_1(\tau)\big) - h\big(\tau, \psi_2(\tau)\big)\| \le T_1\|\psi_1(\tau) - \psi_2(\tau)\|, \tag{2.3}$$

$$\|T\big(\tau, s, \psi_1(s)\big) - T\big(\tau, s, \psi_2(s)\big)\| \le T_2\|\psi_1(\tau) - \psi_2(\tau)\|, \tag{2.4}$$

for every $|\tau - \tau_0| \le 1$, $|s - \tau_0| \le 1$, $\alpha > 0$, $\|u_1\| < \infty$ *and* $\|u_2\| < \infty$. *Then equation* (2.2) *possesses a unique solution.*

Proof. By integrating Eq. (2.2) from 0 to τ, we obtain

$$\begin{aligned} \psi(\tau) &= \psi(\tau_0) + \int_0^\tau h\big(\tau, \psi(\tau)\big)d\tau + \int_0^\tau \Big(\int_0^\tau T\big(\tau, s, \psi(s)\big)ds\Big)d\tau \\ \Rightarrow \psi(\tau) &= \psi(\tau_0) + \int_0^\tau \Big(h\big(\tau, \psi(\tau)\big) + \int_0^\tau T\big(\tau, s, \psi(s)\big)ds\Big)d\tau. \end{aligned} \tag{2.5}$$

If $Y\big(\tau, \psi(\tau)\big) = h\big(\tau, \psi(\tau)\big) + \int_0^\tau T\big(\tau, s, \psi(s)\big)ds$, then equation (2.5) will be as follows:

$$\psi(\tau) = \psi(\tau_0) + \int_0^\tau Y\big(\tau, \psi(\tau)\big)d\tau. \tag{2.6}$$

Now the following conditions hold for equation (2.6):
(1) $\psi(\tau_0)$ is continuous,
(2) due to the continuity of h and T in the same domain, $Y\big(\tau, \psi(\tau)\big)$ is also continuous for $0 \le \tau \le 1$,

(3) $Y\big(\tau,\psi(\tau)\big)$ satisfy the Lipschitz condition.
Consequently, we deduce that

$$\begin{aligned}\|Y\big(\tau,\psi_1(\tau)\big)-Y\big(\tau,\psi_2(\tau)\big)\| &= \|h\big(\tau,\psi_1(\tau)\big)+\int_0^\tau T(\tau,s)V\big(s,\psi_1(s)\big)ds-h\big(\tau,\psi_2(\tau)\big)-\int_0^\tau T(\tau,s)V\big(s,\psi_2(s)\big)ds\|\\ &\le \|h\big(\tau,\psi_1(\tau)\big)-h\big(\tau,\psi_2(\tau)\big)\|+\|\int_0^\tau T(\tau,s)V\big(s,\psi_1(s)\big)ds-\int_0^\tau T(\tau,s)V\big(s,\psi_2(s)\big)ds\|\\ &\le T_1\|\psi_1(\tau)-\psi_2(\tau)\|+T_2\|\psi_1(\tau)-\psi_2(\tau)\|\\ &\le (T_1+\alpha T_2)\|\psi_1(\tau)-\psi_2(\tau)\|. \end{aligned} \tag{2.7}$$

Equation (2.6) is a Volterra integral equation and the criteria of Theorem (2.1) are fulfilled, which implies that the VIDE (2.2) possesses a unique solution. □

3 Fundamental concepts and notations

In this section, we give the definitions of Müntz functions, Block-Pulse functions and some of their properties. Consider $A=\{\mu_0,\mu_1,\cdots\}$ as a complex sequence satisfying the condition $Re(\mu_j)>-\frac{1}{2}$ for all $j\in\mathbb{N}$, and $A_q=\{\mu_0,\mu_1,\cdots,\mu_q\}$. Consider the simple contour Γ and the following function:

$$Q_q(t)=\prod_{j=0}^{q-1}\frac{t+\overline{\mu}_j+1}{t-\mu_j}\frac{1}{t-\mu_q}, \tag{3.1}$$

where Γ encloses all the roots of the denominator in this function.

Definition 3.1. *The Müntz–Legendre polynomials are defined by [46]*

$$g_q(\tau)=g_q(\tau;A_q)=\frac{1}{2\pi i}\oint_\Gamma Q_q(s)\tau^s ds. \tag{3.2}$$

Definition 3.2. *Let $d_q(\tau)$ and $w_q(\tau)$ algebraic polynomials as follows [46]*

$$d_q(\tau)=\sum_{j=0}^{[q/2]}\alpha_j^{(q)}\tau^j,\qquad w_q(\tau)=\sum_{j=0}^{[(q-1)/2]}\beta_j^{(q)}\tau^j. \tag{3.3}$$

Then, the logarithmic Müntz functions $g_q(\tau)$ on the interval $[0,1]$ are defined as follows:

$$g_q(\tau)=d_q(\tau)+w_q(\tau)\ln(\tau),\qquad q=0,1,2,\cdots. \tag{3.4}$$

The coefficients $\alpha_j^{(q)}$ and $\beta_j^{(q)}$ are defined below.

Definition 3.3. *For each $0\le j\le l-1$ and $q=2l$ we have [46]*

$$\alpha_j^{(2l)}=-\binom{l+j}{l}^2\binom{l}{j}^2\left[\frac{2l+1}{2j+1}+2(l-j)\sum_{i=0,i\neq j}^{l-1}\frac{2i+1}{(i-j)(i+j+1)}\right] \tag{3.5}$$

and

$$\beta_j^{(2l)}=-(l-j)\binom{l+j}{l}^2\binom{l}{j}^2. \tag{3.6}$$

For $j=l$ we have

$$\alpha_l^{(2l)}=\binom{2l}{l}^2,\qquad \beta_l^{(2l)}=0. \tag{3.7}$$

For each $0 \le j \le l$ *and* $q = 2l+1$ *we have*

$$\alpha_j^{(2l+1)} = \binom{l+j}{l}^2 \binom{l}{j}^2 \left[\frac{2l+1}{2j+1} + 2(l+j+1) \sum_{i=0, i\neq j}^{l} \frac{2i+1}{(i-j)(i+j+1)} \right] \tag{3.8}$$

and

$$\beta_j^{(2l+1)} = (l+j+1)\binom{l+j}{l}^2 \binom{l}{j}^2. \tag{3.9}$$

Theorem 3.4. *The Müntz functions* $g_q(\tau)$ $(q \ge 0)$ *defined in* (3.4) *possess the characteristic of orthogonality in the range* $[0,1]$ *and contain precisely* q *distinct and simple real roots in this range [46].*

Definition 3.5. *For* $1 \le w \le W$ *the Block-Pulse function on the interval* $[\frac{w-1}{W}, \frac{w}{W})$ *is defined as follows:*

$$\rho_w(\tau) = \begin{cases} 1, & \tau \in [\frac{w-1}{W}, \frac{w}{W}), \\ 0, & \text{otherwise}, \end{cases} \tag{3.10}$$

and for $i, j = 1, \cdots, W$ *these functions are orthogonal i.e.,*

$$\int_0^1 \rho_i(\tau)\rho_j(\tau) = \begin{cases} \frac{1}{W}, & i = j \\ 0, & i \neq j. \end{cases} \tag{3.11}$$

4 Approximation with hybrid functions

This section is devoted to the function approximation using hybrid of Block-Pulse and Müntz functions and its rate of convergence.

4.1 Hybrid functions

Definition 4.1. *In the domain* $[0,1)$*, the hybrid of Block-Pulse and Müntz functions is defined as follows:*

$$\varphi_{wq}(\tau) = \begin{cases} g_q(W\tau - w + 1), & \tau \in [\frac{w-1}{W}, \frac{w}{W}) \\ 0, & \text{otherwise}, \end{cases} \tag{4.1}$$

where $w = 1, \cdots, W$ *and* $q = 0, 1, \cdots Q$ *are the order of Block-Pulse functions and Müntz functions, respectively and* g_q *is the Müntz function defined in* (3.4)*.*

4.2 Function approximation and its convergence rate

Let $\{\varphi_{wq}(\tau)\}$ for $w = 1, \cdots, W$ and $q = 0, 1, \cdots Q$ be a basis on the interval $[0,1]$ such that

$$T = span\{\varphi_{wq}(\tau), w = 1 \cdots W, q = 0, 1, \cdots Q\}, \tag{4.2}$$

and ψ be an integrable function on $[0,1]$. Then, we can approximate ψ with $\widehat{\psi}$ in the structure of a linear combination of the elements of T as follows:

$$\psi(\tau) \simeq \widehat{\psi}(\tau) = \sum_{w=1}^{W} \sum_{q=0}^{Q} c_{wq}\varphi_{wq}(\tau), \tag{4.3}$$

where $\widehat{\psi}$ denotes the best approximation for ψ in T that has the order $W(Q+1)$. Regarding the rate of convergence of this approximation the next theorem can be stated.

Theorem 4.2. *Let $H^u(a,b) = \{\psi \in C^{u-1}([a,b]) : \frac{d\psi^{u-1}}{d\tau} \in L^2(a,b)\}$ and $\psi \in H^u(0,1)$, where u represents an integer with a value of zero or higher. If $u \le W(Q+1)$, then we have*

$$\|\psi - \widehat{\psi}\|_{L^2(0,1)} \le K\big(W(Q+1)\big)^{-u} \|\psi^{(u)}\|_{L^2(0,1)}, \tag{4.4}$$

and if $1 \le \nu \le u$, then we have

$$\|\psi - \widehat{\psi}\|_{H^\nu(0,1)} \le K\big(W(Q+1)\big)^{2\nu-\frac{1}{2}-u} \|\psi^{(u)}\|_{L^2(0,1)}, \tag{4.5}$$

where K represents a constant that depends on the parameter u.

Proof. Let $L_N(\psi)$ be the truncated series of Legendre polynomials for the function ψ. Based on the equation (5.4.11) in [47] for $u \le W(Q+1)$, we have

$$\|\psi - L_N(\psi)\|^2_{L^2(0,1)} \le K\big(W(Q+1)\big)^{-2u} \|\psi^{(u)}\|^2_{L^2(0,1)}. \tag{4.6}$$

Since $\widehat{\psi}$ is the best approximation for ψ, we have

$$\|\psi - \widehat{\psi}\|^2_{L^2(0,1)} = \|\psi - L_N(\psi)\|^2_{L^2(0,1)} \le K\big(W(Q+1)\big)^{-2u} \|\psi^{(u)}\|^2_{L^2(0,1)}. \tag{4.7}$$

Therefore, the argument for the first inequality is completed. The second inequality is proved similarly by using equation (5.5.11) in [47]. □

5 Computational technique

In this section, a computational technique for solving equation (1.1) is derived. We begin by partitioning the interval $[0,1]$ into W equal−length subintervals in the form $I_w = [\frac{w-1}{W}, \frac{w}{W})$, $w = 1, \cdots, W$ with the subinterval length $h = \frac{1}{W}$. Let ψ_w be the numerical solution of equation (1.1) in the subinterval I_w and $s_1, s_2, \cdots, s_q$ be the roots of the Müntz function $g_q(\tau)$ in the interval $[0,1]$ as described in Section 3. We recall that all these roots are simple, distinct and real in $[0,1]$. Then, we transfer these roots to each subinterval I_w for $w = 1 \cdots, W$ by using the following affine transformation:

$$\tau_{w0} = \frac{w-1}{W}, \quad \tau_{wq} = \frac{s_q + w - 1}{W}, \qquad q = 1, \cdots, Q. \tag{5.1}$$

The first note is that the basis functions (4.1) are continuous at the interface of subintervals, so we should impose the additional condition:

$$\psi_w(\frac{w}{W}) = \psi_{w+1}(\frac{w}{W}), \qquad w = 1, \cdots, W. \tag{5.2}$$

Next, we present our collocation strategy for finding the solution to the equation (1.1). The problem is to find $\psi(\tau),\ \tau \in [0,1]$ that satisfies (1.1). In each subinterval $I_w,\ w = 1, \cdots, W$ equation (1.1) is rewritten as follows:

$$G_1\big(\tau, \psi_w(\tau), \frac{d\psi_w(\tau)}{d\tau}\big) = G_2\big(\tau, h(\tau), \psi_w(\tau), \int_0^\tau T(\tau, s) V\big(s, \psi_w(s)\big) ds\big), \qquad \tau \in I_w, \tag{5.3}$$

Since the logarithmic basis functions (4.1) are not defined at $\tau = 0$, instead of approximating the function $\psi_w(\tau)$, we approximate $\frac{d\psi_w(\tau)}{d\tau}$ using this basis as

$$\frac{d\psi_w(\tau)}{d\tau} = \sum_{q=0}^{Q} c_{wq} \varphi_{wq}(\tau), \qquad \tau \in I_w. \tag{5.4}$$

By applying integration to both sides of the equation (5.4) from $\frac{w-1}{W}$ to τ , we get

$$\psi_w(\tau) = \psi_w(\frac{w-1}{W}) + \sum_{q=0}^{Q} c_{wq} \int_{\frac{w-1}{W}}^{\tau} \varphi_{wq}(t) dt, \qquad \tau \in I_w. \tag{5.5}$$

Now, by inserting equations (5.4) and (5.5) into equation (5.3) for $w = 1, \cdots, W$, we obtain

$$G_1\Big(\tau, \sum_{q=0}^{Q} c_{wq} \int_{\frac{w-1}{W}}^{\tau} \varphi_{wq}(t)dt + \psi_w(\frac{w-1}{W}), \sum_{q=0}^{Q} c_{wq}\varphi_{wq}(\tau)\Big) = G_2\Big(\tau, h(\tau), \sum_{q=0}^{Q} c_{wq} \int_{\frac{w-1}{W}}^{\tau} \varphi_{wq}(t)dt + \psi_w(\frac{w-1}{W}), \int_0^{\tau} T(\tau, s) V\big(s, \sum_{q=0}^{Q} c_{wq} \int_{\frac{w-1}{W}}^{s} \varphi_{wq}(t)dt + \psi_w(\frac{w-1}{W})\big)ds\Big). \quad (5.6)$$

By collocating (5.6) at the points (5.1), we arrive at the following collocation conditions:

$$G_1\Big(\tau_{wq}, \sum_{q=0}^{Q} c_{wq} \int_{\frac{w-1}{W}}^{\tau_{wq}} \varphi_{wq}(t)dt + \psi_w(\frac{w-1}{W}), \sum_{q=0}^{Q} c_{wq}\varphi_{wq}(\tau_{wq})\Big) = G_2\Big(\tau_{wq}, h(\tau_{wq}), \sum_{q=0}^{Q} c_{wq} \int_{\frac{w-1}{W}}^{\tau_{wq}} \varphi_{wq}(t)dt + \psi_w(\frac{w-1}{W}), \int_0^{\tau_{wq}} T(\tau_{wq}, s) V\big(s, \sum_{q=0}^{Q} c_{wq} \int_{\frac{w-1}{W}}^{s} \varphi_{wq}(t)dt + \psi_w(\frac{w-1}{W})\big)ds\Big). \quad (5.7)$$

Then, we replace the integral from 0 to τ_{wq} for $w = 1, \cdots, W$ and $q = 0, \cdots, Q$ in equation (5.7) with the sum of two separate integrals from 0 to $\frac{w-1}{W}$ and from $\frac{w-1}{W}$ to τ_{wq} as follows:

$$G_1\Big(\tau_{wq}, \sum_{q=0}^{Q} c_{wq} \int_{\frac{w-1}{W}}^{\tau_{wq}} \varphi_{wq}(t)dt + \psi_w(\frac{w-1}{W}), \sum_{q=0}^{Q} c_{wq}\varphi_{wq}(\tau_{wq})\Big) = G_2\Big(\tau_{wq}, h(\tau_{wq}), \sum_{q=0}^{Q} c_{wq} \int_{\frac{w-1}{W}}^{\tau_{wq}} \varphi_{wq}(t)dt + \psi_w(\frac{w-1}{W}), \int_0^{\frac{w-1}{W}} T(\tau_{wq}, s) V\big(s, \sum_{q=0}^{Q} c_{wq} \int_{\frac{w-1}{W}}^{s} \varphi_{wq}(t)dt + \psi_w(\frac{w-1}{W})\big)ds + \int_{\frac{w-1}{W}}^{\tau_{wq}} T(\tau_{wq}, s) V\big(s, \sum_{q=0}^{Q} c_{wq} \int_{\frac{w-1}{W}}^{s} \varphi_{wq}(t)dt + \psi_w(\frac{w-1}{W})\big)ds\Big), \quad (5.8)$$

in which, the following integral can be calculated using the approximate results of the previous subintervals:

$$\int_0^{\frac{w-1}{W}} T(\tau_{wq}, s) V\big(s, \sum_{q=0}^{Q} c_{wq} \int_{\frac{w-1}{W}}^{s} \varphi_{wq}(t)dt + \psi_w(\frac{w-1}{W})\big)ds = \int_0^{\frac{1}{W}} T(\tau_{wq}, s) V\big(s, \sum_{q=0}^{Q} c_{wq} \int_{\frac{w-1}{W}}^{s} \varphi_{wq}(t)dt + \psi_w(\frac{w-1}{W})\big)ds + \int_{\frac{1}{W}}^{\frac{2}{W}} T(\tau_{wq}, s) V\big(s, \sum_{q=0}^{Q} c_{wq} \int_{\frac{w-1}{W}}^{s} \varphi_{wq}(t)dt + \psi_w(\frac{w-1}{W})\big)ds + \cdots + \int_{\frac{w-2}{W}}^{\frac{w-1}{W}} T(\tau_{wq}, s) V\big(s, \sum_{q=0}^{Q} c_{wq} \int_{\frac{w-1}{W}}^{s} \varphi_{wq}(t)dt + \psi_w(\frac{w-1}{W})\big)ds. \quad (5.9)$$

Therefore, equation (5.8) will be rewritten as

$$
\begin{aligned}
G_1\Big(\tau_{wq}, \sum_{q=0}^{Q} c_{wq} \int_{\frac{w-1}{W}}^{\tau_{wq}} \varphi_{wq}(t)dt + \psi_w(\frac{w-1}{W}), \sum_{q=0}^{Q} c_{wq}\varphi_{wq}(\tau_{wq})\Big) \quad = \quad & G_2\Big(\tau_{wq}, h(\tau_{wq}), \sum_{q=0}^{Q} c_{wq} \int_{\frac{w-1}{W}}^{\tau_{wq}} \varphi_{wq}(t)dt + \psi_w(\frac{w-1}{W}), \\
& \int_{0}^{\frac{1}{W}} T(\tau_{wq}, s)V\big(s, \sum_{q=0}^{Q} c_{wq} \int_{\frac{w-1}{W}}^{s} \varphi_{wq}(t)dt + \psi_w(\frac{w-1}{W})\big)ds + \\
& \int_{\frac{1}{W}}^{\frac{2}{W}} T(\tau_{wq}, s)V\big(s, \sum_{q=0}^{Q} c_{wq} \int_{\frac{w-1}{W}}^{s} \varphi_{wq}(t)dt + \psi_w(\frac{w-1}{W})\big)ds + \cdots \\
& + \int_{\frac{w-2}{W}}^{\frac{w-1}{W}} T(\tau_{wq}, s)V\big(s, \sum_{q=0}^{Q} c_{wq} \int_{\frac{w-1}{W}}^{s} \varphi_{wq}(t)dt + \psi_w(\frac{w-1}{W})\big)ds + \\
& \int_{\frac{w-1}{W}}^{\tau_{wq}} T(\tau_{wq}, s)V\big(s, \sum_{q=0}^{Q} c_{wq} \int_{\frac{w-1}{W}}^{s} \varphi_{wq}(t)dt + \psi_w(\frac{w-1}{W})\big)ds\Big).
\end{aligned} \tag{5.10}
$$

All the integral terms in (5.10) can be calculated utilizing the Gauss–Legendre integration approach. To achieve this, first we transform the intervals $[\frac{w-1}{W}, \frac{w}{W}]$ and $[\frac{w-1}{W}, \tau_{wq}]$ to the interval $[-1, 1]$ by using the following affine transformations:

$$
s = \frac{t}{2W} + \frac{2w-1}{2W}, \qquad s = \frac{t}{2}(\tau_{wq} - \frac{w-1}{W}) + \frac{w-1+W\tau_{wq}}{2W}, \qquad w = 1, \cdots, W, \qquad t \in [-1, 1]. \tag{5.11}
$$

Utilizing the Gauss–Legendre quadrature rule for equation (5.9), yields:

$$
\begin{aligned}
\int_{0}^{\frac{w-1}{W}} T(\tau_{wq}, s)V\big(s, \sum_{q=0}^{Q} c_{wq} \int_{\frac{w-1}{W}}^{s} \varphi_{wq}(t)dt + \psi_w(\frac{w-1}{W})\big)ds \quad = \quad & \sum_{j=1}^{k} \frac{1}{2W}\omega_j T(\tau_{wq}, \frac{t_j+1}{2W})V\big(\frac{t_j+1}{2W}, \\
& \sum_{q=0}^{Q} c_{wq} \int_{\frac{w-1}{W}}^{\frac{t_j+1}{2W}} \varphi_{wq}(t)dt + \psi_w(\frac{w-1}{W})\big) + \\
& \sum_{j=1}^{k} \frac{1}{2W}\omega_j T(\tau_{wq}, \frac{t_j+3}{2W})V\big(\frac{t_j+3}{2W}, \\
& \sum_{q=0}^{Q} c_{wq} \int_{\frac{w-1}{W}}^{\frac{t_j+3}{2W}} \varphi_{wq}(t)dt + \psi_w(\frac{w-1}{W})\big) \\
& + \cdots + \sum_{j=1}^{k} \frac{1}{2W}\omega_j T(\tau_{wq}, \frac{t_j+2W-3}{2W})V\big(\frac{t_j+2W-3}{2W}, \\
& \sum_{q=0}^{Q} c_{wq} \int_{\frac{w-1}{W}}^{\frac{t_j+2W-3}{2W}} \varphi_{wq}(t)dt + \psi_w(\frac{w-1}{W})\big),
\end{aligned} \tag{5.12}
$$

where $\omega_j, t_j, j = 1, \cdots, k$ represent the associated weights and points for Gauss–Legendre integration approach and k

is the order of Legendre polynomial $L_k(\tau)$. Finally, equation (5.10) will be approximated as follows:

$$
\begin{aligned}
G_1\Big(\tau_{wq}, \sum_{q=0}^{Q} c_{wq} \int_{\frac{w-1}{W}}^{\tau_{wq}} \varphi_{wq}(t)dt + \psi_w(\frac{w-1}{W}), \sum_{q=0}^{Q} c_{wq}\varphi_{wq}(\tau_{wq})\Big) \quad = \quad & G_2\Big(\tau_{wq}, h(\tau_{wq}), \sum_{q=0}^{Q} c_{wq} \int_{\frac{w-1}{W}}^{\tau_{wq}} \varphi_{wq}(t)dt + \\
& \psi_w(\frac{w-1}{W}), \sum_{j=1}^{k} \frac{1}{2W}\omega_j T(\tau_{wq}, \frac{t_j+1}{2W}) V\big(\frac{t_j+1}{2W}, \\
& \sum_{q=0}^{Q} c_{wq} \int_{\frac{w-1}{W}}^{\frac{t_j+1}{2W}} \varphi_{wq}(t)dt + \psi_w(\frac{w-1}{W})\big) + \\
& \sum_{j=1}^{k} \frac{1}{2W}\omega_j T(\tau_{wq}, \frac{t_j+3}{2W}) V\big(\frac{t_j+3}{2W}, \\
& \sum_{q=0}^{Q} c_{wq} \int_{\frac{w-1}{W}}^{\frac{t_j+3}{2W}} \varphi_{wq}(t)dt + \psi_w(\frac{w-1}{W})\big) + \cdots + \\
& \sum_{j=1}^{k} \frac{1}{2W}\omega_j T(\tau_{wq}, \frac{t_j+2W-3}{2W}) V\big(\frac{t_j+2W-3}{2W}, \\
& \sum_{q=0}^{Q} c_{wq} \int_{\frac{w-1}{W}}^{\frac{t_j+2W-3}{2W}} \varphi_{wq}(t)dt + \psi_w(\frac{w-1}{W})\big) + \\
& \sum_{j=1}^{k} \frac{\tau_{wq}-\frac{w-1}{W}}{2}\omega_j T\big(\tau_{wq}, \frac{t_j}{2}(\tau_{wq}-\frac{w-1}{W}) + \frac{w-1+W\tau_{wq}}{2W}\big) \\
& V\big(\frac{t_j}{2}(\tau_{wq}-\frac{w-1}{W}) + \frac{w-1+W\tau_{wq}}{2W}, \sum_{q=0}^{Q} c_{wq} \\
& \int_{\frac{w-1}{W}}^{\frac{t_j}{2}(\tau_{wq}-\frac{w-1}{W})+\frac{w-1+W\tau_{wq}}{2W}} \varphi_{wq}(t)dt + \psi_w(\frac{w-1}{W})\big)\Big). \qquad (5.13)
\end{aligned}
$$

Equation (5.13) for $w = 1, \cdots, W$ and $q = 0, \cdots, Q$ results in an algebraic equations system characterized by an order of $W(Q+1)$ which is solvable via Newton's iterative technique for the coefficients c_{wq}. By finding the coefficients c_{wq} and substituting them into (4.3), the numerical solution of VIDE (1.1) is obtained.

In the sequel, we describe our algorithm that uses the components described above:

Step 1: Input

Consider the VIDE (1.1) and the initial condition $\psi(\tau_0) = \xi$. Divide the interval $[0, 1]$ into W number of equal-length subintervals and consider the equation (1.1) in each subinterval I_w as given below

$$
G_1\big(\tau, \psi_w(\tau), \frac{d\psi_w(\tau)}{d\tau}\big) = G_2\big(\tau, h(\tau), \psi_w(\tau), \int_0^{\tau} T(\tau, s)V\big(s, \psi_w(s)\big)ds\big), \qquad \tau \in I_w, \qquad w = 1, \cdots, W. \qquad (5.14)
$$

Choose the number of Müntz functions Q to be used for function approximation.

Step 2: Generation of hybrid functions and solution approximation

Generate hybrid functions $\varphi_{wq}(\tau)$ for $q = 0, 1, \cdots, Q$ $w = 1, \cdots, W$ as defined in Section 4. These basis functions are not defined at $\tau = 0$, so approximate $\frac{d\psi_w(\tau)}{d\tau}$ using this basis as

$$
\frac{d\psi_w(\tau)}{d\tau} = \sum_{q=0}^{Q} c_{wq}\varphi_{wq}(\tau), \qquad \tau \in I_w. \qquad (5.15)
$$

Integrate both sides of the equation (5.15) from $\frac{w-1}{W}$ to τ, to get

$$\psi_w(\tau) = \psi_w(\frac{w-1}{W}) + \sum_{q=0}^{Q} c_{wq} \int_{\frac{w-1}{W}}^{\tau} \varphi_{wq}(t)dt, \qquad \tau \in I_w. \tag{5.16}$$

Step 3: Substitution of expansions

Insert equations (5.15) and (5.16) into equation (5.14) for $w = 1, \cdots, W$.

Step 4: Set up the system of algebraic equations

Consider the collocation points

$$\tau_{w0} = \frac{w-1}{W}, \quad \tau_{wq} = \frac{s_q + w - 1}{W}, \qquad q = 1, \cdots, Q, \qquad w = 0, 1, \cdots, W, \tag{5.17}$$

where $s_1, s_2, \cdots, s_q$ are the roots of the Müntz function. Collocate the equation raised from Step 3 at the collocation points (5.17) and form a system of algebraic equations in terms of the coefficients c_{wq}.

Step 5: Construction of the approximate solution

Utilize the Newton's iterative method to solve the system of Step 4. Substitute the computed coefficients c_{wq} back into the relation (5.16) to get the approximate solution $\widehat{\psi}_w(\tau)$ for the equation (1.1).

6 Stability assessment

In this section, we investigate the stability of the proposed numerical approach. The stability issue means that the error caused by the starting error is controllable in long computations. To this end, let $< \cdot, \cdot >_{L^2(I_w)}$ and $< \cdot, \cdot >_{I_w,Q}$ denotes the inner product and discrete inner product on the subinterval I_w, respectively. For simplicity of statement, consider the following VIDE:

$$\frac{d\psi(\tau)}{d\tau} = G\Big(\tau, h(\tau), \psi(\tau), \int_0^{\tau} T(\tau, s)V\big(s, \psi(s)\big)ds\Big), \qquad \tau \in \Gamma = [0, 1], \qquad \psi(\tau_0) = \psi_0, \tag{6.1}$$

under the condition

$$\left[G\Big(\tau, h(\tau), \psi(\tau), \int_0^{\tau} T(\tau, s)V\big(s, \psi(s)\big)ds\Big) - G\Big(\tau, h(\tau), y(\tau), \int_0^{\tau} T(\tau, s)V(s, y(s))ds\Big)\right](u - y) \leq 0. \tag{6.2}$$

By recalling that, in the present method the original interval $\Gamma = [0, 1]$ is divided into W subintervals I_w such that

$$I_w = [\tau_{w-1}, \tau_w] = [\frac{w-1}{W}, \frac{w}{W}], \qquad h = \frac{1}{W}, \qquad w = 1, \cdots, W, \tag{6.3}$$

our purpose is to show that the following definition holds true for the present method.

Definition 6.1. *A numerical method for the integro-differential equation* (6.1) *is called RN–stable, if the numerical approximations* $\widehat{\psi}(\tau)$ *and* $\widehat{y}(\tau)$ *with* $\widehat{\psi}(\tau_0) = \widehat{\psi}_0$ *and* $\widehat{y}(\tau_0) = \widehat{y}_0$*, satisfy the following relation:*

$$|\widehat{\psi}(\tau_w) - \widehat{y}(\tau_w)| \leq |\widehat{\psi}_0 - \widehat{y}_0|, \qquad w = 1, \cdots, W. \tag{6.4}$$

Let $\widehat{\psi}_w(\tau)$ and $\widehat{y}_w(\tau)$ be the numerical solutions on the subinterval I_w corresponding to the initial values $\widehat{\psi}(\tau_0) = \widehat{\psi}_0$ and $\widehat{y}(\tau_0) = \widehat{y}_0$. Also, let $\widehat{e}_w(\tau) = \widehat{\psi}_w(\tau) - \widehat{y}_w(\tau)$. By substituting $\widehat{\psi}_w(\tau)$ and $\widehat{y}_w(\tau)$ into Eq. (6.1) and then subtract the results, we get

$$\begin{aligned}
&\frac{d\widehat{e}_w(\tau)}{d\tau} = \frac{d\widehat{\psi}_w(\tau)}{d\tau} - \frac{d\widehat{y}_w(\tau)}{d\tau} = \\
&G\Big(\tau, h(\tau), \widehat{\psi}_w(\tau), \int_0^{\tau} T(\tau, s)V\big(s, \widehat{\psi}_w(s)\big)ds\Big) - \\
&G\Big(\tau, h(\tau), \widehat{y}_w(\tau), \int_0^{\tau} T(\tau, s)V\big(s, \widehat{y}_w(s)\big)ds\Big),
\end{aligned} \tag{6.5}$$

where

$$\widehat{e}_w(\tau_{w-1}) = \widehat{e}_{w-1}(\tau_{w-1}), \qquad \widehat{e}_1(\tau_0) = \widehat{\psi}_0 - \widehat{y}_0, \qquad w = 1, \cdots, W. \tag{6.6}$$

Multiplying both sides of Eq. (6.5) by $\widehat{e}_w(t_{wq})w_{wq}$, where w_{wq} and t_{wq} are respectively the Gauss–Legendre quadrature weights and points on I_w, and summing the results for $0 \leq q \leq Q$ and utilizing (6.2), we arrive at

$$\begin{aligned} &< \frac{d\widehat{e}_w}{d\tau}, \widehat{e}_w >_{I_w,Q} = \\ &< G\Big(\tau, h(\tau), \widehat{\psi}_w(\tau), \int_0^\tau T(\tau,s)V\big(s, \widehat{\psi}_w(s)\big)ds\Big) - \\ &G\Big(\tau, h(\tau), \widehat{y}_w(\tau), \int_0^\tau T(\tau,s)V\big(s, \widehat{y}_w(s)\big)ds\Big), \widehat{e}_w >_{I_w,Q} \leq 0. \end{aligned} \tag{6.7}$$

Since $\widehat{e}_w(\tau)$ and $\frac{d\widehat{e}_w}{d\tau}$ are polynomials of degree up to Q on I_w, one can formulate

$$(\widehat{e}_w.\frac{d\widehat{e}_w}{d\tau})(\tau) := \sum_{i=1}^{2Q} k_{w,i}\tau^i, \tag{6.8}$$

where $k_{w,i}$ is a constant. Using lemma 2 in [48], we have

$$\int_{I_w} \tau^i d\tau \leq h_{w,i} \sum_{q=0}^{i} w_{wq} t_{wq}^i, \tag{6.9}$$

where $h_{w,i}$ is a positive constant. Now, by ralation (6.9) and (6.7), we get

$$< \frac{d\widehat{e}_w}{d\tau}, \widehat{e}_w >_{L^2(I_w)} \leq < \frac{d\widehat{e}_w}{d\tau}, \widehat{e}_w >_{I_w,Q} \leq 0. \tag{6.10}$$

On the other hand, we have

$$\big(\widehat{e}_w(\tau_w)\big)^2 - \big(\widehat{e}_w(\tau_{w-1})\big)^2 = < \frac{d\widehat{e}_w}{d\tau}, \widehat{e}_w >_{L^2(I_w)}, \tag{6.11}$$

hence, we conclude that

$$\big(\widehat{e}_w(\tau_w)\big)^2 - \big(\widehat{e}_w(\tau_{w-1})\big)^2 \leq 0. \tag{6.12}$$

Consequently, for $w = 1, \cdots, W$ we have that

$$|\widehat{\psi}(\tau_w) - \widehat{y}(\tau_w)| \leq |\widehat{\psi}(\tau_{w-1}) - \widehat{y}(\tau_{w-1})|, \tag{6.13}$$

which implies

$$|\widehat{\psi}(\tau_w) - \widehat{y}(\tau_w)| \leq |\widehat{\psi}_0 - \widehat{y}_0|. \tag{6.14}$$

Relation (6.14) proves the numerical stability of the presented method.

7 Error assessment

Here, we confirm the convergence of the suggested approach and we obtain its convergence rate for the VIDE (1.1). In what follows, let E_N be the residual error of the presented collocation approach.

Theorem 7.1. *Let $\psi \in H^u(0,1)$, where u is a non-negative integer and $T' = max_{\tau,s\in[0,1]\times[0,1]}|T(\tau,s)|$. Assume that the functions $V, \frac{d\psi(\tau)}{d\tau}, \int_0^\tau T(\tau,s)V\big(\psi(s)\big)ds$ fulfill the Lipschitz condition using the Lipschitz constants η_1, η_2, η_3, respectively. Then, we have*

$$\|E_N\|_{L^2(0,1)} \leq (\eta_2 + \eta_1 + T'\eta_1\eta_3)^{-u} K\big(W(Q+1)\big)^{-u} \|\psi^{(u)}\|_{L^2(0,1)} + \eta_1 K(W(Q+1))^{(2\nu-\frac{1}{2}-u)} \|\psi^{(u)}\|_{L^2(0,1)}. \tag{7.1}$$

Proof. According to the definition of E_N, it follows that

$$\|E_N\|_{L^2(0,1)} = \left\| \frac{d\widehat{\psi}_w}{d\tau} - h(\tau) - \int_0^\tau T(\tau,s)V\big(\widehat{\psi}_w(s)\big)ds - \frac{d\psi}{d\tau} + h(\tau) + \int_0^\tau T(\tau,s)V\big(\psi(s)\big)ds \right\|. \tag{7.2}$$

The triangle inequality together with the Lipschitz conditions, imply

$$\|E_N\|_{L^2(0,1)} \leq \eta_1 \| \frac{d\psi}{d\tau} - \frac{d\widehat{\psi}_w}{d\tau} \|_{L^2(0,1)} + (\eta_2 + \eta_1 + T'\eta_1\eta_3)\|\psi - \widehat{\psi}_w\|_{L^2(0,1)}. \tag{7.3}$$

According to the Theorem 4.2, we can write

$$\left\| \frac{d\psi}{d\tau} - \frac{d\widehat{\psi}_w}{d\tau} \right\|_{L^2(0,1)} \leq \|\psi - \widehat{\psi}_w\|_{H^\nu(0,1)} \leq K\big(W(Q+1)\big)^{2\nu-\frac{1}{2}-u}\|\psi^{(u)}\|_{L^2(0,1)}, \tag{7.4}$$

and finally

$$\|E_N\|_{L^2(0,1)} \leq (\eta_2 + \eta_1 + T'\eta_1\eta_3)^{-u} K\big(W(Q+1)\big)^{-u}\|\psi^{(u)}\|_{L^2(0,1)} + \eta_1 K\big(W(Q+1)\big)^{(2\nu-\frac{1}{2}-u)}\|\psi^{(u)}\|_{L^2(0,1)}, \tag{7.5}$$

as desired. □

Remark 7.2. *We note that by increasing W and Q, the obtained error bound goes to zero that shows the converges of the method.*

8 Illustrative examples

To validate the effectiveness, high precision and efficiency of the proposed approach, we provide three examples and compare our findings with those obtained by the methods described in [14] and [15]. All examples have been solved using the Maple 2020 software package and is measured with an accuracy of 50 decimal places. All the computations are carried out by means of a laptop with the configuration: Intel(R) Core(TM) i5 CPU, 4.00G RAM and 2.20GHz, with 64 bits operation system.

Example 8.1. *As the first example consider the VIDE [14]*

$$\psi'(\tau) = \tau cos(\tau) + cos(\tau) + \frac{1}{2}\tau cos(\tau)sin(\tau) - \frac{1}{2}\tau^2 + \int_0^\tau \big(\tau\psi^2 - cos(\tau)\big)ds, \qquad \tau \in [0,1], \tag{8.1}$$

with the initial condition

$$\psi(0) = 0. \tag{8.2}$$

The exact solution is to this problem is

$$\psi(\tau) = sin(\tau). \tag{8.3}$$

To solve this equation with the proposed method, we will follow the steps below.

- *First, we simplify equation* (8.1) *as follows*

$$\psi'(\tau) = cos(\tau) + \frac{1}{2}\tau cos(\tau)sin(\tau) - \frac{1}{2}\tau^2 + \tau\int_0^\tau \big(\psi^2\big)ds, \qquad \tau \in [0,1]. \tag{8.4}$$

- *Now, we devide the interval* $[0,1]$ *into* W *equal-length subintervals and in each subinterval* I_w *we set*

$$\frac{d\psi_w(\tau)}{d\tau} = \sum_{q=0}^{Q} c_{wq}\varphi_{wq}(\tau), \qquad \tau \in I_w, \tag{8.5}$$

where $\varphi_{wq}(\tau)$ *is the hybrid function defined in section 4.*

- *Integrating both sides of the relation* (8.5) *yields*

$$\psi_w(\tau) = \sum_{q=0}^{Q} c_{wq} \int_{\frac{w-1}{W}}^{\tau} \varphi_{wq}(t)dt + \psi(\frac{w-1}{W}), \qquad \tau \in I_w. \tag{8.6}$$

- *By substituting equations* (8.5) *and* (8.6) *into equation* (8.4) *and collocating the resulting equation at the points defined in* (5.1) *for* $w = 1, \cdots, W$ *and* $q = 0, \cdots, Q$ *we have*

$$\sum_{q=0}^{Q} c_{wq}\varphi_{wq}(\tau_{wq}) = cos(\tau_{wq}) + \frac{1}{2}\tau_{wq}cos(\tau_{wq})sin(\tau_{wq}) - \frac{1}{2}(\tau_{wq})^2 + \tau_{wq}\int_0^{\tau_{wq}} ((\sum_{q=0}^{Q} c_{wq}\int_{\frac{w-1}{W}}^{\tau_{wq}} \varphi_{wq}(t)dt + \psi(\frac{w-1}{W}))^2)ds, \tag{8.7}$$

  where to calculate the integral 0 to τ_{wq}*, relations* (5.8)-(5.13) *from Section 6 are utilized.*

- *Now, we have* $W(Q+1)$ *algebraic equations with the unknown coefficients* c_{wq} *for* $w = 1 \cdots, W$ *and* $q = 0, \cdots, Q$*, which is solved using Maple software and the numerical solution of equation* (8.1) *is obtained using* (4.3).

2 presents the absolute errors of the proposed method for $W = 10, 20$ *and* $Q = 2, 4, 9, 15$ *and the methods presented in the references [14] and [15]. Also, the graphs of the absolute error functions for* $Q = 2, 4, 9, 15$ *and* $W = 10$ *are depicted in 1. As can be seen in 2, the absolute errors of the proposed method are less than that of the other two methods. Furthermore, as the value of* W *increases, the absolute errors in the proposed method decrease demonstrating the convergence by increasing the number of subintervals. In the plots of absolute error functions in 1 and 2, it can be observed that as the value of* Q *increases, the absolute errors decrease, highlighting the superior accuracy of the proposed method.*

Example 8.2. *The second VIDE is expressed as follows [14]*

$$\psi'(\tau) = \frac{-1}{8}\tau^9 - \frac{2}{7}\tau^8 + \frac{1}{6}\tau^7 + \frac{2}{5}\tau^6 - \frac{1}{4}\tau^5 + 2\tau + 1 + \int_0^{\tau} (\tau s^3\psi^2)ds, \tag{8.8}$$

under the initial condition

$$\psi(0) = -1. \tag{8.9}$$

The exact solution is

$$\psi(\tau) = \tau^2 + \tau - 1. \tag{8.10}$$

To solve this equation with the proposed method, by applying the same strategy as in the Example 8.1, we get $W(Q+1)$ equations which can be resolved to determine the unknown coefficients $c_{wq}, w = 1 \cdots, W$, $q = 0, \cdots, Q$. The results for several values of Q and W are presented in 3. In this table, the absolute errors of the proposed method and the methods from references [14] and [15] are presented for $Q = 2, 3, 4$ and $W = 10, 20$. It is evident that the accuracy of the proposed method is substantially higher than that of the other two methods. The graphs of the absolute error functions are shown in 2 for $Q = 2, 3, 4$ and $W = 10$.

Example 8.3. *The last example is VIDE below [14]*

$$\psi'(\tau) = \frac{-1}{10}\tau^{10} + \frac{1}{3}\tau^9 - \frac{3}{8}\tau^8 - \frac{1}{7}\tau^7 + \frac{2}{3}\tau^6 - \frac{2}{5}\tau^5 + 3\tau^2 - \tau + \int_0^{\tau} (\psi^3 - \psi^2 - \psi)ds, \tag{8.11}$$

subject to the initial condition

$$\psi(0) = 1. \tag{8.12}$$

The exact solution is

$$\psi(\tau) = \tau^3 - \tau^2 + 1. \tag{8.13}$$

Table 2: Values of absolute error corresponding to Example 8.1 for $Q = 2, 4, 9, 15$

Q	Method in [14]	Method in [15]	Present method with $W = 10$	Present method with $W = 20$
2	9.0×10^{-3}	3.0×10^{-2}	2.5×10^{-4}	7.0×10^{-5}
4	9.0×10^{-5}	2.0×10^{-4}	9.0×10^{-7}	1.0×10^{-7}
9	1.0×10^{-6}	1.0×10^{-11}	2.0×10^{-14}	3.5×10^{-16}
15	4.0×10^{-8}	9.0×10^{-22}	2.5×10^{-23}	4.0×10^{-26}

Table 3: Values of absolute error corresponding to Example 8.2 for $Q = 2, 3, 4$

Q	Method in [14]	Method in [15]	Present method with $W = 10$	Present method with $W = 20$
2	1.7×10^{-3}	1.0×10^{-9}	8.0×10^{-4}	2.0×10^{-4}
3	2.0×10^{-4}	8.0×10^{-10}	6.0×10^{-50}	1.0×10^{-49}
4	4.5×10^{-5}	1.0×10^{-9}	1.6×10^{-49}	1.0×10^{-49}

To solve this equation, by applying similar operations as in the previous two examples we get $W(Q+1)$ equations, which can be solved to find the the unknown coefficients $c_{wq}, w = 1 \cdots, W, q = 0, \cdots, Q$. The results for several values of Q and $W = 10, 20$ are demonstrated in 4. In this table, it is still observed that as the values of Q and W increase, the absolute error in proposed method decreases. Additionally, by comparing the absolute errors of the three methods presented in the 4, it can be noted that the accuracy of the proposed method is higher than that of methods [14] and [15]. The graphs of the absolute error functions for $Q = 2, 4, 6, 8$ and $W = 10, 20$ are shown in 3. In this figure, a significant reduction in the absolute error of the equation with increasing values of Q compared to reference method [14] and [15] is clearly observed, demonstrating the superiority of the proposed method over method [14] and [15].

In 5, the execution time for solving all three mentioned equations using the proposed method is presented for different values of Q and W, demonstrating that the execution time is reasonable for reaching highly accurate approximate solutions. Although it also depends on the level of the nonlinearity of the problem.

Table 4: Values of absolute error corresponding to Example 8.3 for $Q = 2, 4, 6, 8$

Q	Method in [14]	Method in [15]	Present method with $W = 10$	Present method with $W = 20$
2	4.2×10^{-4}	4.0×10^{-1}	1.0×10^{-3}	2.5×10^{-4}
4	7.6×10^{-6}	6.0×10^{-2}	5.0×10^{-6}	6.0×10^{-7}
6	1.0×10^{-6}	6.0×10^{-5}	2.0×10^{-49}	2.0×10^{-49}
8	2.4×10^{-7}	4.0×10^{-6}	2.5×10^{-49}	1.0×10^{-49}

Table 5: The execution time for examples 8.1, 8.2 and 8.3 for different values of Q and W

	Q	Execution time (s) with $W = 10$	Execution time (s) with $W = 20$
Example 8.1	2	0.8	1.5
	4	2.0	4.2
	9	26.6	48.9
	15	367.0	1084.4
Example 8.2	2	0.9	1.5
	3	2.8	5.5
	4	5.2	10.7
Example 8.3	2	0.9	1.7
	4	5.7	12.3
	6	64.0	124.3
	8	300.6	629.9

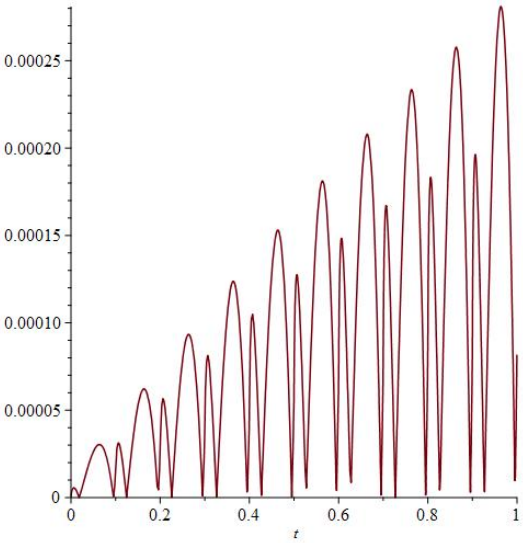

(a) $Q = 2$

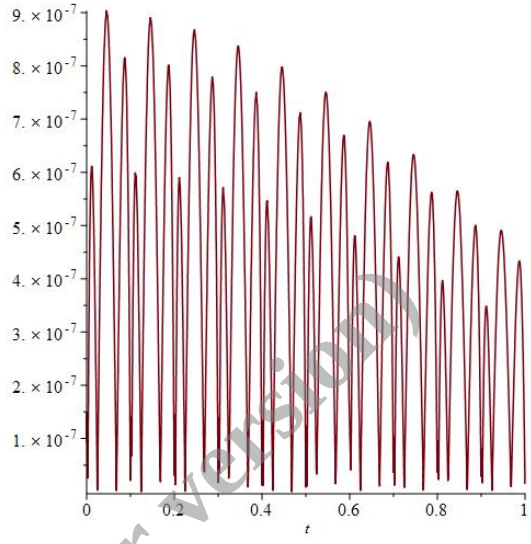

(b) $Q = 4$

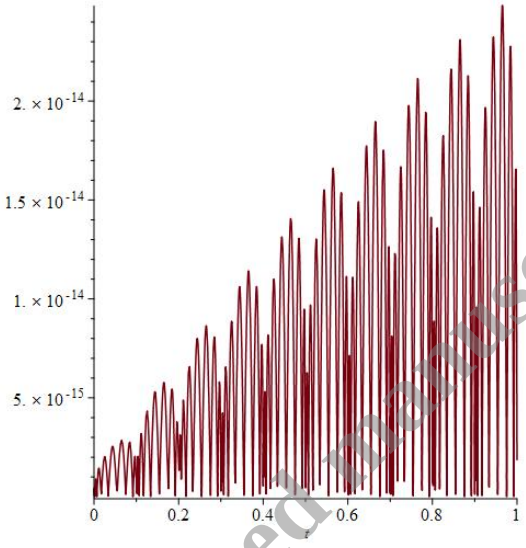

(c) $Q = 9$

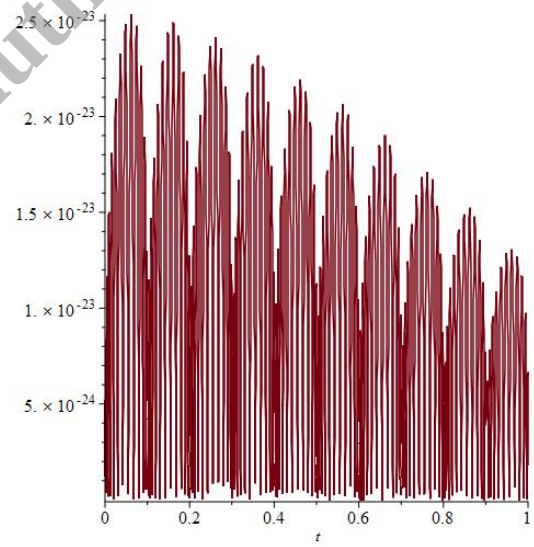

(d) $Q = 15$

Figure 1: Values of absolute error corresponding to Example 8.2 for $W = 10$

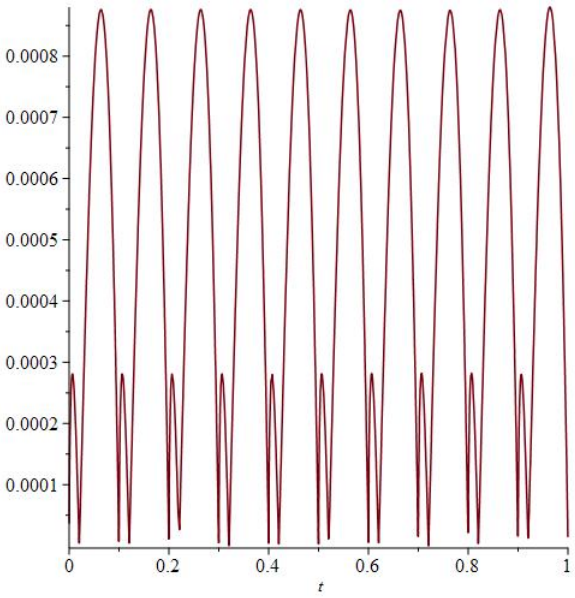

(a) $Q = 2$

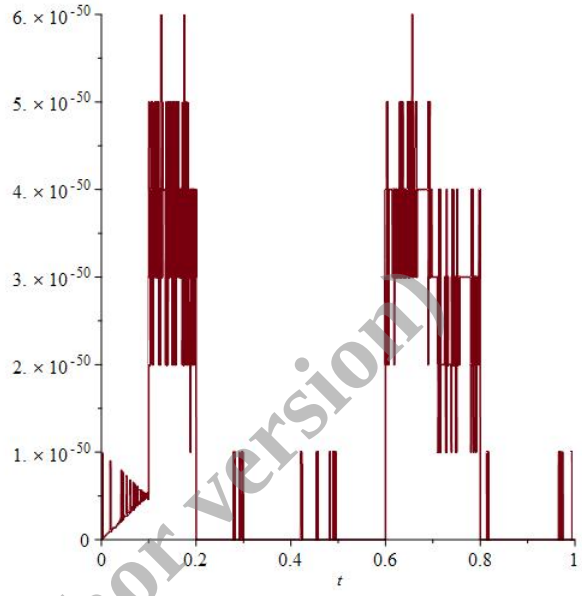

(b) $Q = 3$

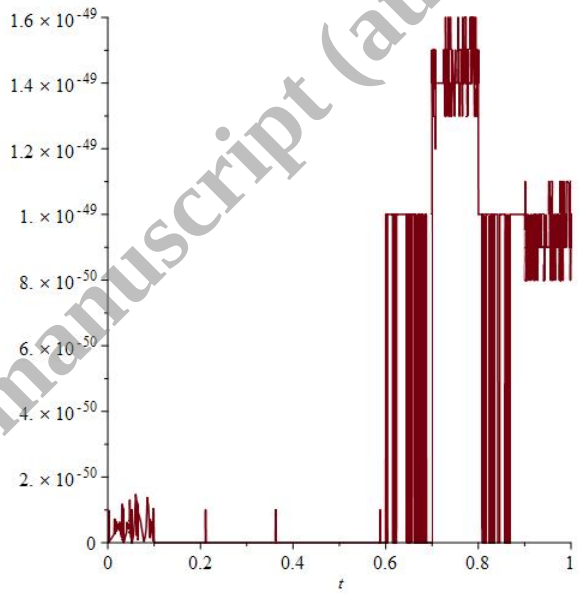

(c) $Q = 4$

Figure 2: Values of absolute error corresponding to Example 8.2 for $W = 10$

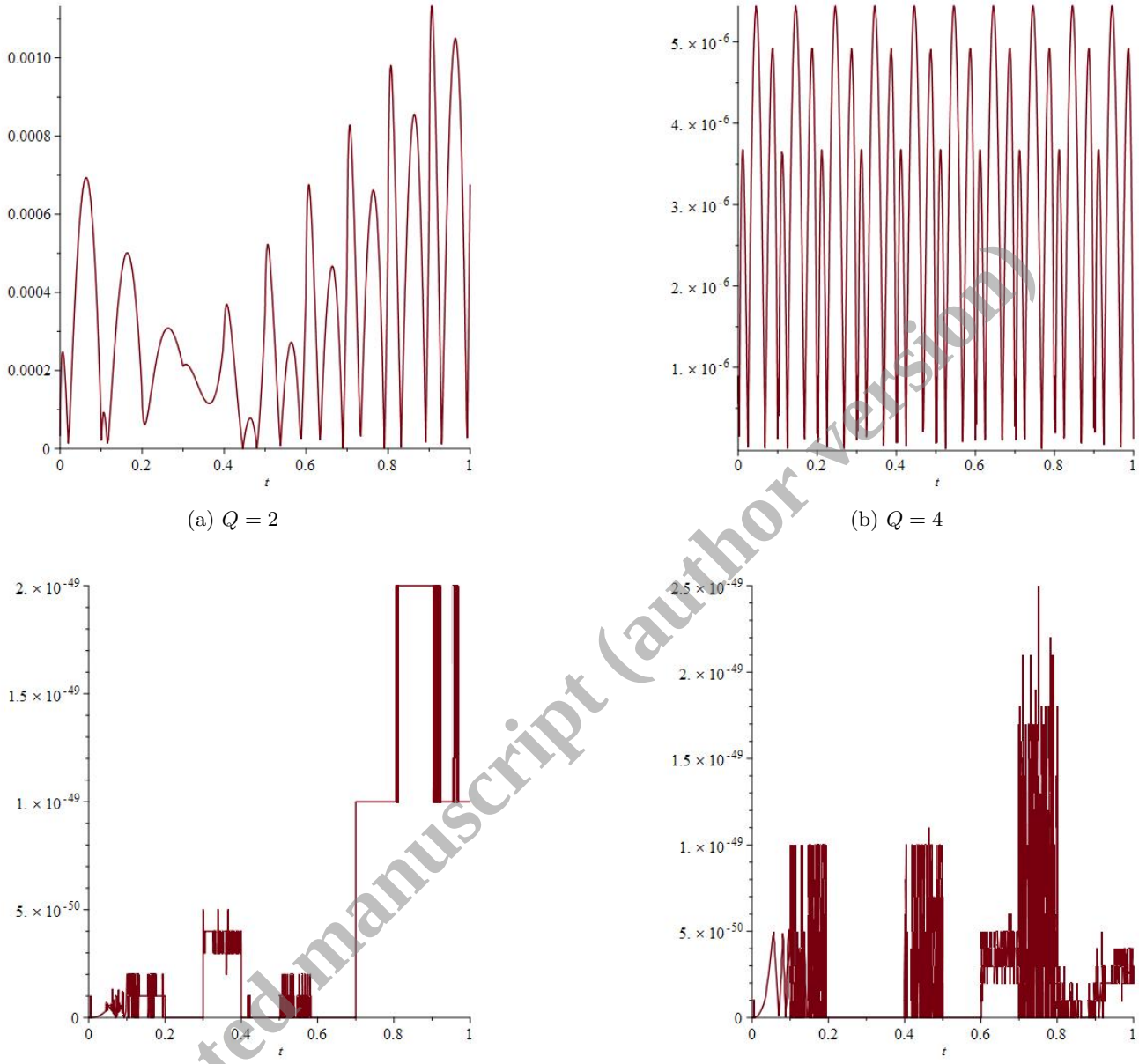

(a) $Q = 2$ (b) $Q = 4$

(c) $Q = 6$ (d) $Q = 8$

Figure 3: Values of absolute error corresponding to Example 8.3 for $W = 10$

9 Conclusions and future research directions

In this article, a new basis has been constructed by combining Block-Pulse functions with logarithmic Müntz functions. Then we introduced a new collocation approach for solving VIDEs, by utilizing the constructed hybrid basis and the Müntz nodes as the collocation points. Numerical results demonstrated the numerical stability and spectral accuracy of the method, which are in agreement with the theoretical results presented in Sections 6 and 7. In addition, it was shown that this method has superiority over the hat functions approach and the Legendre polynomials method and its execution time for reaching at least the machine precision is reasonable especially for moderate number of subintervals and basis functions.

Considering the extensive applications of real world fractional order equations, for future researches, the method

presented in this article can be utilized to solve equations such as second-order two-dimensional symmetric sequential fractional integro-differential equations, fractional non-isothermal reaction-diffusion model equations in a spherical catalyse, sequential fractional wave equations and fractional system of Riccati equations. Additionally, the proposed approach can be applied to solve other multidimensional VIDEs and fractional VIDEs.

References

[1] E. A. Az-Zo-bi, W. A. AlZoubi, L. Akinyemi, M. Senol, I. W. Alsaraireh, and M. Mamat. Abundant closed-form solitons for time-fractional integro–differential equation in fluid dynamics. *Optical and Quantum Electronics*, 53(3):132, 2021.

[2] E. Khairullin and A. Azhibekova. A general boundary value problem for heat and mass transfer equations with high order normal derivatives in boundary conditions. *AIP Conference Proceedings*, 2325(1):020011, 2021.

[3] R. Pourgholi, R. Azimi, and A. Tahmasbi. Application of Tau approach for solving integro-differential equations with a weakly singular kernel. *Iranian Journal of Mathematical Sciences and Informatics*, 16(1):145–168, 2021.

[4] A. Bidari, F. D. Saei, M. Baghmisheh, and T. Allahviranloo. A new Jacobi Tau method for fuzzy fractional Fredholm nonlinear integro-differential equations. *Soft Computing*, 25(8):5855–5865, 2021.

[5] V. Finek. Wavelet-Galerkin method for integro-differential equations. *AIP Conference Proceedings*, 2425, 2022.

[6] W. M. Abd-Elhameed and Y. H. Youssri. Numerical solutions for Volterra-Fredholm Hammerstein integral equations via second kind Chebyshev quadrature collocation algorithm. *Advances in Applied Mathematics*, 24(1):129–141, 2014.

[7] E. H. Doha, Y. H. Youssri, and M. A. Zaky. Spectral solutions for differential and integral equations with varying coefficients using classical orthogonal polynomials. *Bulletin of the Iranian Mathematical Society*, 45(2):527–555, 2019.

[8] R. M. Hafez and Y. H. Youssri. Chebyshev collocation treatment of Volterra-Fredholm integral equation with error analysis. *Arabian Journal of Mathematics*, 9(2):471–480, 2020.

[9] L. Hongyan, J. Huang, and W. Zhang. Numerical algorithm based on extended barycentric Lagrange interpolant for two dimensional integro-differential equations. *Applied Mathematics and Computation*, 396(125931), 2021.

[10] R. M. Hafez and Y. H. Youssri. Spectral Legendre-Chebyshev treatment of 2d linear and nonlinear mixed Volterra-Fredholm integral equation. *Mathematical Sciences Letters*, 9(2):37–47, 2020.

[11] S. Kumar, J. J. Nieto, and B. Ahmad. Chebyshev spectral method for solving fuzzy fractional Fredholm-Volterra integro-differential equation. *Mathematics and Computers in Simulation*, 192:501–513, 2022.

[12] R. Amin, I. Mahariq, K. Shah, M. Awais, and F. Elsayed. Numerical solution of the second order linear and nonlinear integro-differential equations using haar wavelet method. *Arab Journal of Basic and Applied Sciences*, 28(1):12–20, 2021.

[13] N. Khongnual and W. Thadee. Solutions of Fredholm integro-differential equations by using a hybrid of Block-Pulse functions and taylor polynomials. *Songklanakarin Journal of Science and Technology*, 43(1):127–132, 2021.

[14] K. M. Jehad and A. R. Khudair. Integro-differential equations: Numerical solution by a new operational matrix based on fourth-order hat functions. *Partial Differential Equations in Applied Mathematics*, 8(100529), 2023.

[15] M. O. Olayiwola, A. F. Adebısı, and Y. S. Arowolo. Application of legendre polynomial basis function on the solution of volterra integro-differential equations using collocation method. *Cankaya University Journal of Science and Engineering*, 17(1):41–51, 2020.

[16] X. Li and Z. Rui. Physics-informed deep ai simulation for fractal integro-differential equation. *Fractals*, 32(01):2450022, 2024.

[17] G. Mehdiyeva, V. Ibrahimov, and M. Imanova. On some comparison of the multistep hybrid methods and their application solving of the volterra integro-differential equations. *Journal of Physics: Conference Series*, 1334(1):012007, 2019.

[18] A. Jafarian, F. Rostami, A. K. Golmankhaneh, and D. Baleanu. Using anns approach for solving fractional order volterra integro-differential equations. *International Journal of Computational Intelligence Systems*, 10(1):470–480, 2017.

[19] R. Saneifard, A. Jafarian, N. Ghalami, and S. Measoomy Nia. Extended artificial neural networks approach for solving two-dimensional fractional-order volterra-type integro-differential equations. *Information Sciences*, 612:887–897, 2022.

[20] T. Allahviranloo, A. Jafarian, R. Saneifard, N. Ghalami, S. Measoomy Nia, F. Kiani, U. Fernandez-Gamiz, and S. Noeiaghdam. An application of artificial neural networks for solving fractional higher-order linear integro-differential equations. *Boundary Value Problems*, 2023(1):74, 2023.

[21] L. Yuan, Yi-Qing N., Xiang-Yun D., and Shuo H. A-pinn: Auxiliary physics informed neural networks for forward and inverse problems of nonlinear integro-differential equations. *Journal of Computational Physics*, 462:111260, 2022.

[22] E. H. Doha, M. A. Abdelkawy, A. Z. M. Amin, and D. Baleanu. Spectral technique for solving variable-order fractional volterra integrodi×erential equations. *Numerical Methods for Partial Differential Equations*, 34(5):1659–1677, 2018.

[23] B. Nemati Saray. An efficient algorithm for solving volterra integro-differential equations based on alpert's multi-wavelets galerkin method. *Journal of Computational and Applied Mathematics*, 348:453–465, 2019.

[24] T. S. Gutleb. A fast sparse spectral method for nonlinear integro-differential volterra equations with general kernels. *Advances in Computational Mathematics*, 47(3):42, 2021.

[25] O. Abu Arqub. Adaptation of reproducing kernel algorithm for solving fuzzy fredholm–volterra integrodifferential equations. *Neural Computing and Applications*, 28(7):1591–1610, 2017.

[26] O. Abu Arqub, J. Singh, and M. Alhodaly. Adaptation of kernel functions-based approach with atangana baleanu caputo distributed order derivative for solutions of fuzzy fractional volterra and fredholm integrodifferential equations. *Mathematical Methods in the Applied Sciences*, 46(7):7807–7834, 2023.

[27] H. Badawi, O. Abu Arqub, and N. Shawagfeh. Well-posedness and numerical simulations employing legendre-shifted spectral approach for caputo fabrizio fractional stochastic integrodifferential equations. *International Journal of Modern Physics C*, 34(06):2350070, 2023.

[28] H. Badawi, O. Abu Arqub, and N. Shawagfeh. Existence, uniqueness, and collocation solutions using the shifted legendre spectral method for the hilfer fractional stochastic integro-differential equations regarding stochastic brownian motion. *Results in Applied Mathematics*, 24:100504, 2024.

[29] G. V. Badalyan. Generalization of Legendre polynomials and some of their applications. *Akad. Nauk. Armyan. SSR Izv. Fiz.-Mat. Estest. Tekhn. Nauk*, 8(5):1–28, 1955.

[30] A. K. Taslakyan. Some properties of Legendre quasipolynomials with respect to a Müntz system. *Mathematics*, 2:179–189, 1984.

[31] P. C. McCarthy, J. E. Sayre, and B. L. R. Shawyer. Generalized Legendre polynomials. *Journal of Mathematical Analysis and Applications*, 177(2):530–537, 1993.

[32] P. Borwein, T. Erdelyi, and J. Zhang. Müntz systems and orthogonal Müntz−Legendre polynomials. *American Mathematical Society*, 342(2):523–542, 1994.

[33] B. Dankovic, G. V. Milovanovic, and S. Lj. Rancic. Malmquist and Müntz orthogonal systems and applications. *Inner Product Spaces and Applications*, pages 22–4l, 1997.

[34] G. V. Milovanovic, B. Dankovic, and S. Lj. Rancic. Some Müntz orthogonal systems. *Journal of Computational and Applied Mathematics*, 99:299–310, 1998.

[35] S. Akhlaghi, M. Tavassoli Kajani, and M. Allame. Application of Müntz orthogonal functions on the solution of the fractional Bagley-Torvik equation using collocation method with error stimate. *Advances in Mathematical Physics*, 2023:5520787, 2023.

[36] S. Esmaeili, M. Shamsi, and Y. Luchko. Numerical solution of fractional differential equations with a collocation method based on Müntz polynomials. *Computers & Mathematics with Applications*, 62(3):918–929, 2011.

[37] M. Pourbabaee and A. Saadatmandi. A new operational matrix based on Müntz-Legendre polynomials for solving distributed order fractional differential equations. *Mathematics and Computers in Simulation (MATCOM)*, 194(C):210–235, 2022.

[38] P. Mokhtari, F. Ghoreishi, and H. Srivastava. The Müntz−Legendre Tau method for fractional differential equations. *Applied Mathematiacal Modeling*, 40(2):671–684, 2016.

[39] H. R. Marzban. A generalization of Müntz−Legendre polynomials and its implementation in optimal control of nonlinear fractional delay systems. *Chaos, Solitons & Fractals*, 158(112093), 2022.

[40] N. Negarchi and K. Nouri. Numerical solution of Volterra–Fredholm integral equations using the collocation method based on a special form of the Müntz−Legendre polynomials. *Journal of Computational and Applied Mathematics*, 344:15–24, 2018.

[41] F. Ghanbari, P. Mokhtary, and K. Ghanbari. Numerical solution of a class of fractional order integro-differential algebraic equations using Müntz–jacobi Tau method. *Journal of Computational and Applied Mathematics*, 362:172–184, 2019.

[42] M. Bahmanpour, M. Tavassoli Kajani, and M. Maleki. Solving Fredholm integral equations of the first kind using Müntz wavelets. *Applied Numerical Mathematics*, 143:159–171, 2019.

[43] F. Saemi, H. Ebrahimi, and M. Shafiee. An effective scheme for solving system of fractional Volterra–Fredholm integro-differential equations based on the Müntz–Legendre wavelets. *Journal of Computational and Applied Mathematics*, 374(112773), 2020.

[44] P. Linz. A method for solving nonlinear volterra integral equations of the second kind. *Mathematics of Computation*, 23(107):595–599, 1969.

[45] F. G. Tricomi. Integral equations. *Courier corporation*, 5, 1985.

[46] G. V. Milovanovic. Müntz orthogonal polynomials and their numerical evaluation. *Applications and Computation of Orthogonal Polynomials*, 131:179–194, 1999.

[47] C. Canuto, M. Y. Hussaini, A. Quarteroni, and T. A. Zang. *Spectral methods*, volume 285. Springer, 2006.

[48] M. Maleki and A. Davari. Fractional retarded differential equations and their numerical solution via a multistep collocation method. *Applied Numerical Mathematics*, 143:203–222, 2019.